Nozzle-free electrospinning of Polyvinylpyrrolidone/Poly(glycerol sebacate) fibrous scaffolds for skin tissue engineering applications

Nozzle-free electrospinning of Polyvinylpyrrolidone/Poly(glycerol sebacate) fibrous scaffolds for skin tissue engineering applications

Antonios Keirouz[a, b]

Giuseppino Fortunato[b]

Zhang Mei[a, c]

Anthony Callanan[c]

Norbert Radacsi[a, *]

n.radacsi@ed.ac.uk

[a]The School of Engineering, Institute for Materials and Processes, The University of Edinburgh, King's Buildings, Edinburgh, EH9 3FB, United Kingdom

[b]Empa, Swiss Federal Laboratories for Materials Science and Technology, Laboratory for Protection and Physiology, St. Gallen, CH-9014, Switzerland

[c]The School of Engineering, Institute for Bioengineering, The University of Edinburgh, The King's Buildings, Edinburgh, EH9 3JL, United Kingdom

*Corresponding author.

In brief: A nozzle-free electrospinning device was designed for the fabrication of biocompatible PVP:PGS nonwoven fibrous mats, which presented compelling mechanical properties adjustable apropos to the blend ratio and the PVP's molecular weight.

Abstract

A novel composite for skin tissue engineering applications by use of blends of Poly(vinylpyrrolidone) (PVP) and Poly (glycerol sebacate) (PGS) was fabricated via the scalable nozzle-free electrospinning technique. The formed PVP:PGS blends were morphologically, thermochemically and mechanically characterized. The morphology of the developed fibers correlated to the blend ratio. The tensile modulus appeared to be affected by the concentration of PGS within the blends, with an apparent decrease in the elastic modulus of the electrospun mats and an exponential increase of the elongation at break. Ultraviolet (UV) crosslinking of the composite fibers significantly decreased the construct's wettability and stabilized the formed fiber mats, which was indicated by contact angle measurements. *In vitro* examination showed good viability and proliferation of human dermal fibroblast cells. The present findings provide valuable insights for tuning the elastic properties of electrospun material by incorporating this unique elastomer as a promising future candidate for skin substitute constructs.

Keywords: PGS; PVP; UV; Nozzle-free electrospinning; Elastic; Polymer

1 Introduction

Skin tissue engineering (TE) requires the development of biomimetic scaffolds that provide all the necessary biochemical mechanisms and topographical cues for efficient skin regeneration [1,2].

Nanostructured materials are favorable towards the fabrication of porous fibrous meshes as they permit the development of structures that closely resemble the native extracellular matrix (ECM) where cells can adhere, proliferate, freely migrate and induce neovascularization [3,4]. Presently, the majority of the skin substitute models are non-resorbable scaffolds based on allographs [3,5]. Nonetheless, much focus is being directed to the development of bioresorbable scaffolds that convey all the requirements to act as short-term matrices, capable of being slowly resorbed by the newly formed tissue [6].

Among the spectrum of biomaterials available, utilizing natural and synthetic polymers remain at the center of attention [7]. Poly(glycerol sebacate) (PGS) is a recently discovered *Federal Drug Administration* (FDA) approved semi-crystalline thermoset, with promising applications for soft tissue engineering [8,9]. PGS is synthesized via the polycondensation of glycerol and sebacic acid to form a pre-polymer, which can be further covalently crosslinked [10,11]. Poly(polyol sebacate)-derived polymers such as PGS refer to a family of ester-bonded elastomers formed via the polycondensation of polyol alcohols, containing multiple hydroxyl groups (e.g., glycerol, isomalt, xylitol) and the dicarboxylic acid present in sebacic acid [12,13].

PGS is a very attractive biomaterial as it exhibits tailored mechanical properties and bioresorbability pertinent to varying the polycondensation parameters and stoichiometry, which correlate to the surface degradability of its ester linkages [14,15]. As a result, PGS has been exponentially investigated *in vitro* and *in vivo* on studies focusing on cardiac [16–18], vascular [19,20], cartilage [9,21], nerve guidance [22,23], retina [24–26], adipose [27], skin [28,29], as well as a potential drug carrier [30,31].

Among the available fabrication techniques such as freeze-drying, solvent casting, and particulate leaching, reactive injection molding, phase separation, and self-assembly – electrospinning has been contemplated as an ideal candidate for fabricating, cost-effective, porous, random or aligned fibrous scaffolds [32,33]. Electrospun fibers facilitate an increased surface-to-volume area and porosity, which makes them appealing towards the development of biomimetic scaffolds with an ECM architecture that promotes cellular attachments [34]. Furthermore, by employing a nozzle-free electrospinning device for the fabrication, rather than a conventional needle-based setup, it is possible to sustain an increased fiber production rate, making it feasible to scale-up the process [35]. A nozzle-free electrospinning setup could be automatized by the development of a user interface that can control all the key electrospinning parameters of the process (humidity, temperature, working distance, and potential difference). A pump system can maintain a sustained feeding of polymer solution level, and the nanofiber collection can be arranged in a roll-to-roll fiber deposition process.

Electrospinning thermosets such as PGS can be challenging since uncured pre-polymer forms tend to be very viscous, whereas their cured counterparts are insoluble in most organic solvents, owing to a low glass transition temperature (T_g), eventually forming non-fibrous plasticized scaffolds [36,37]. Consequently, PGS cannot be electrospun without conjugating with polymers that can promptly form fibers [36,38]. Several polymers including poly(caprolactone) (PCL) [9,34,39], gelatin [40,41], poly(vinyl alcohol) (PVA) [36,42], poly(L-lactide) (PLLA) [11] and poly(ethylene oxide) (PEO) [43] have been used as carrier polymers to facilitate the development of PGS fibers. Poly(vinylpyrrolidone) (PVP) is a hydrophilic polymer used as a polar stabilizer, capable of readily forming fibers and was chosen to facilitate with the spinnability of the PGS [44].

The human skin is a non-linear, anisotropic and viscoelastic organ, where distinct areas differ significantly regarding mechanical behavior [45]. Hence, the mechanical properties of specific sites, based on the anatomical attributes of the human body, must be taken into consideration when developing such constructs.

In this study, reported for the first time, we fabricated PVP:PGS blended fibers via the nozzle-free electrospinning technique, which was subsequently cross-linked using ultraviolet (UV) radiation.

The ability of the elastomer to tune the mechanical properties of two distinct molecular weight (M_w) PVP polymers was investigated. The structure and morphological characteristics and the mechanical properties of the developed scaffolds were analyzed using scanning electron microscopy (SEM), Fourier-transform infrared spectroscopy (FTIR), differential scanning calorimetry (DSC), tensile testing and water contact angle measurements. The biocompatibility of the PVP:PGS scaffolds was carried out by seeding the scaffolds with immortalized human dermal fibroblasts (HDF) using Alamar blue viability assay.

2 Materials and methods

2.1 Materials

PVP (M_w=360,000 and 1,300,000) was purchased from Sigma-Aldrich, UK. Sebacic acid (≥98%, M_w = 202.20) and glycerol (≥99.5%, ~~M_w~~ M_w = 92.09) were purchased from Alfa-Aesar, UK. Other chemicals and solvents such as absolute ethanol (99.8%) Acros Organics, dimethylformamide (DMF) (99%) Alfa Aesar and 1,1,1,3,3,3-Hexafluoro-2-propanol (HFIP) (99%) Fluorochem were utilized without further processing.

Immortalized human skin fibroblast cells (HDF-hTERT) were donated from the MRC Centre for Reproductive Health, Edinburgh, UK. High glucose, pyruvate, Dulbecco's Modified Eagle Medium (DMEM), fetal bovine serum albumin (FBS), non-essential amino acids (NEAA), penicillin-streptomycin and Hanks' Balanced Salt Solution (HBSS) were purchased from Thermo-Fisher Scientific, UK. Glutaraldehyde (GA), hexamethyldisilazane (HDMS), and sucrose were purchased from Alfa-Aesar, UK.

2.2 PGS synthesis and polymer blending

PGS was synthesized based on the original method published by Wang et al., with selected modifications [10]. Briefly, equimolar amounts of sebacic acid and glycerol were thoroughly mixed in a three-neck flask under N_2 for 24 h at 120 °C to obtain the pre-polymer, pPGS (Fig. 1). The pressure was then reduced to 40 mTorr, and the reaction was continued for a further 48 h in a vacuum oven at 120 °C (Fig. 1).

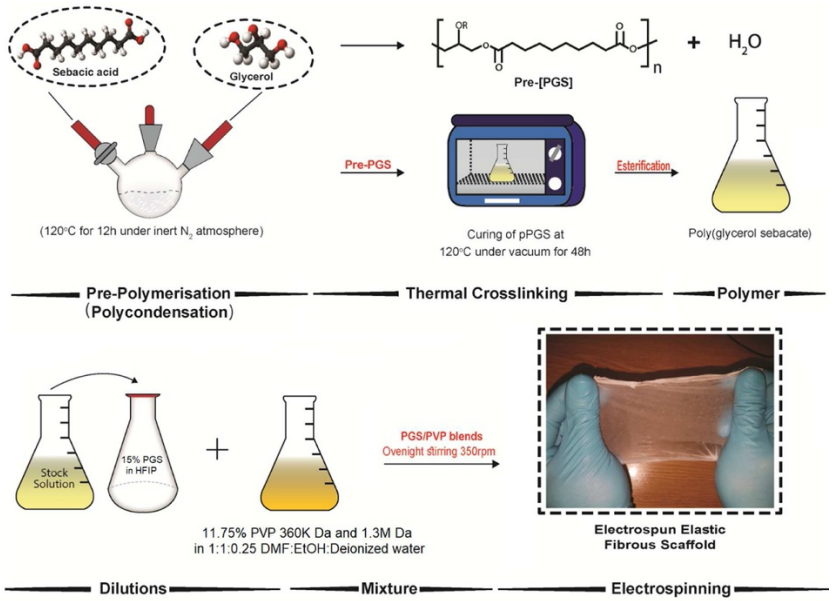

Fig. 1 Schematic illustration of the PGS synthesis, and solution preparation that results in flexible, stretchable skin-like nanofibrous mats.

alt-text: Fig 1

The PGS was dissolved in HFIP to form 15~~%~~ % w/v polymer solution. PVP with molar masses of 360 k and 1.3 M g/mol were dissolved separately in a solvent system encompassing 1:1:0.25 v/v ratio of DMF: Ethanol: distilled H_2O to form 11.75~~%~~ % w/v polymer solution. All solutions were stirred overnight at room temperature, before blending. Afterwards, blends of 100:0, 95:5, 90:10, 80:20, 70:30, 40:60 and 50:50 w/w ratio of PVP:PGS were prepared and mixed for 12 h prior to electrospinning (Table 1).

Table 1 Summary of the electrospinning solutions parameters and blending ratios.

alt-text: Table 1

Polymer blend	Ratio (PVP:PGS) [w/w]
I. 11.75% PVP (w/v) (M_w=1,300,000) + 15% (w/v) PGS **&** **II.** 11.75% (w/v) PVP (M_w=360,000) + 15% (w/v) PGS	100:0
	95:5
	90:10
	80:20
	70:30
	60:40
	50:50

2.3 Scaffold fabrication and processing

A custom-built nozzle-free electrospinning device comprised of a rotating stainless steel cylinder electrode inside a Teflon pool where the polymer solution blends were immersed and a biased rotating collector electrode under constant hot air flow (working distance 15 cm, airflow 450 L min^{-1}, temperature 150 °C). A potential difference of 60 kV DC was applied between the two rotating electrodes (+30 kV on the electrode inside the pool and −30 kV on the

collector electrode), resulting in the formation of multiple Taylor cones on the rotating electrode surface immersing in the solution bath, from which jets stretched to form fibers in an upwards motion. A cellulose-based paper (commercial baking paper) was used to collect the fibers. All experiments were carried out under ambient conditions at a relative humidity ranging from 30–40% and room temperature of 18–22 °C. Fig. 2 gives a schematic overview of the fabrication process.

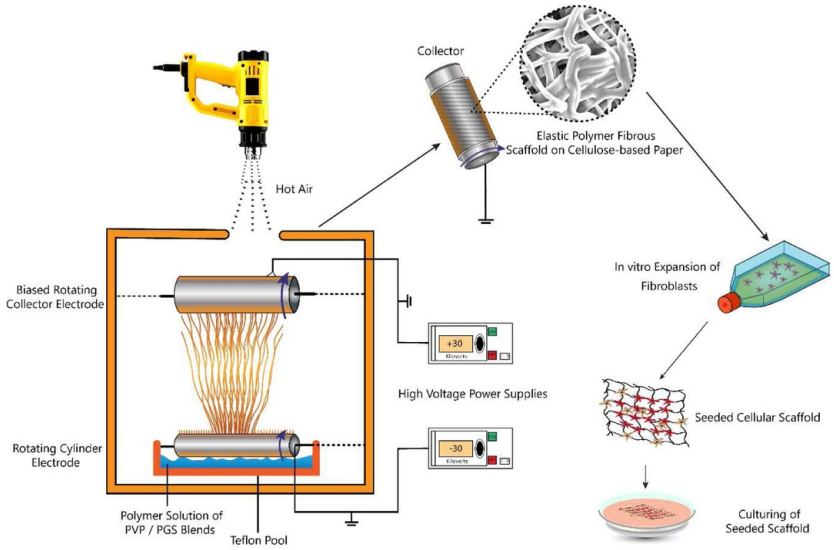

Fig. 2 Schematic figure of the nozzle-free electrospinning procedure, and the seeding of the cellular scaffold and cell culturing of the seeded scaffolds.

alt-text: Fig 2

UV irradiation of the PVP:PGS scaffolds was conveyed to induce crosslinking of the two distinct electrospun polymers. Solutions containing 0.2 to 1% w/w Riboflavin were also prepared as an enzymatic photosensitizer [46,47]. The membranes were irradiated in the dose range of 5 kGy for 30 and 60 min at a 15 cm distance between the exposed surface and the halogen lamp, using a 254 nm UV lamp (Novascan, USA).

2.4 Physicochemical characterization

The fiber morphology, mean fiber diameter and porosity of the electrospun composite membranes were determined by scanning electron microscopy, SEM (JEOL, JSM 6010 PLUS, Japan). 10 nm thick gold was sputter coated on the surface of the fibrous mats.

The chemical composition of the raw polymer material and that of the fibers were determined by attenuated total reflectance, Fourier-transform infrared spectroscopy (ATR-FTIR) (Perkin-Elmer). The wavelength ranged between 4000 and 650 cm^{-1} at 2 cm^{-1} resolution, where 32 scans per specimen were obtained. The specimens were first vacuumed dried and mixed with KBr to form pallets under ambient conditions.

The surface chemistry of the electrospun scaffolds for each blend was analyzed by X-ray photoelectron spectroscopy (XPS) taken with a PHI 5000 VersaProbe II (USA) using an Al Kα X-ray source. The energy resolution of the spectrometer was set to 0.8 eV/step at a pass-energy of 187.85 eV for the survey scans. Carbon 1 s at 284.5 eV was used as a calibration reference to correct for charge effects. Elemental compositions were determined using instrument dependent atom sensitivity factors. The photoelectron-transitions C1s, O1s, and N1s were selected to determine the elemental concentrations. Data analysis was performed by use of CasaXP software (Casa Software Ltd, United Kingdom).

Differential scanning calorimeter (DSC) measurements were performed at a heating rate of 10 °C/min (DSC9000, Perkin-Elmer, USA) to measure the melting temperature (T_m) and crystallization point (T_c) of the composite membranes. The enthalpy of heat fusion was determined based on the first heating curve and held for 5 min at 240 °C. The samples were sealed in aluminum crucibles and were examined at a temperature ranging from −60 °C to 240 °C.

Static water contact angle measurements were obtained to determine the wettability properties of the PVP:PGS membranes after UV treatment (DSA100, Kruss, Germany). Specimens were wetted by allowing a 5 µL deionized

water droplet to settle at the center of each fiber mat.

2.5 Mechanical testing

The mechanical properties of the electrospun PVP:PGS scaffolds were determined by uniaxial tensile testing (Instron universal testing machine 3367, UK). The scaffolds were cut using a customized mold into dog-shaped specimens with an outer area (115 mm (length) x 25 mm (width)) and inner area (84 mm(length) x 6 mm (width)), based on the ISO standards on determining tensile properties of films and sheets [48]. The thickness of each electrospun mat was measured with a high-precision digital micrometer. The specimens were tested in axial tensile loading on a 100 N cell at a constant strain rate of 50 mm/min (5% of non-load value), where the fracture stress and strain curves were plotted. The Young's modulus was calculated based on the linear section of the stress-strain curve.

2.6 Scaffold cell seeding and viability measurements

The cell attachment properties onto the scaffolds were observed by SEM (JEOL, JSM 6010 PLUS, Japan). The scaffolds were punched into 8 mm circular pieces, and sterilized with 70% (v/v) ethanol for 24 h. The scaffolds were first rinsed in deionized water for 24 h, followed by soaking in DMEM for 48 h. Cells were then seeded onto scaffolds in 20 µL suspension in 48-well tissue culture plates, with a density of 1×10^5 cells/scaffold. The seeded scaffolds were kept still for 2 h after seeding and were then incubated (37 °C/5% CO_2) for 4 h before adding 400 µL of fresh media in each well. The media were replaced in a manner of 50/50 fresh/old every other day. After incubation for 1, 4, and 5 days the cell-seeded electrospun mats collected and washed with warm HBSS, and fixed with 3% (v/v) glutaraldehyde at 4 °C overnight. The scaffolds were then washed thoroughly with SEM buffer consisting of 0.01 M PBS and 0.1 M sucrose, and gradually dehydrated in ethanol (35%, 50%, 60%, 70%, 95%, and 100%, v/v), for 15 min at each concentration. After, the scaffolds were chemically dried with HDMS overnight. The dried scaffolds were sputter-coated with 8 nm Au and then submitted to SEM for cell attachment observations.

To appraise the proliferation rate of the cells on the scaffolds, Alamar blue assay, a quantitative test that measures the conversion rate of resazurin (blue) to resorufin (red) by viable cells, was carried out 1, 3, 5 and 7 days after seeding.

The scaffolds were punched in 3 mm circular pieces and treated for 24 h in 70% ethanol, 24 h in deionized water and 48 h in Dulbecco's Modified Eagle Medium (DMEM). The pinched scaffolds were then placed in a 96-well plate, and 2.5×10^5 HDF-hTERTs were seeded per electrospun mat at a 20 µL suspension for 6 h prior to adding 100 µL DMEM high glucose, pyruvate, doped with 10% fetal bovine serum (FBS), 1% non-essential amino acids, 1% L-glutamine and 1% penicillin-streptomycin (v/v).

The cell proliferation rate (CPR) was calculated based on $CPR = OD_E/OD_c$ x 100% with OD_E the absorbance rate of the cell-seeded serum and ODc, the absorbance density of the negative control group. Two readings quantified the fluorescence, using a microplate reader (Modulus™ II, Turner BioSystems, USA), by placing the aliquots in a dark Enzyme-linked immunosorbent assay ELISA plate and reading at $\lambda = 490$ nm (excitation) and $\lambda = 510$–570 nm (emission).

3 Results and discussion

3.1 Fiber morphology assessment

As PGS is intrinsically difficult to electrospin, PVP was used as a carrier polymer. Fig. 3 shows the SEM micrographs of 1.3 M and 360 k g/mol PVP for the various (w/w) blends of PVP:PGS that were electrospun. For all of the blends, the concentration of PGS is 15% (w/v), whereas the PVP is 11.75% (w/v). Morphologically, the fiber network displays a random ECM-like architecture. The cotton candy-like morphology of the PVP mats transformed into paraffin-like scaffolds as the concentration of PGS gradually increased within the blends. A more gelatinized morphology with less homogenous fiber appearance is present for the blends with increased PGS concentration, where the scaffolds appear to form porous gel-like mats under which PGS seems to coat the PVP fibers during the electrospinning process. The mean fiber diameter of the PVP was 0.97 ± 0.65 µm and 0.85 ± 0.58 µm for 1.3 M and 360 k g/mol, respectively (Fig. 4). The mean fiber diameter between the blends did not appear to be significantly affected by increasing the PGS concentration; with the 50:50 PVP:PGS blend ratio, the fibers appear to have completely merged, forming a gel as shown in Fig. 5. The average porosity of the scaffolds ranged between 40–60%, regardless of the blend ratio or the M_w of the PVP. Nonetheless, the mean pore area appeared to gradually decrease from 8.52 ± 0.65 μm^2 for the pure PVP scaffolds to 0.70 ± 0.18 μm^2 for the 50:50 PVP:PGS blend.

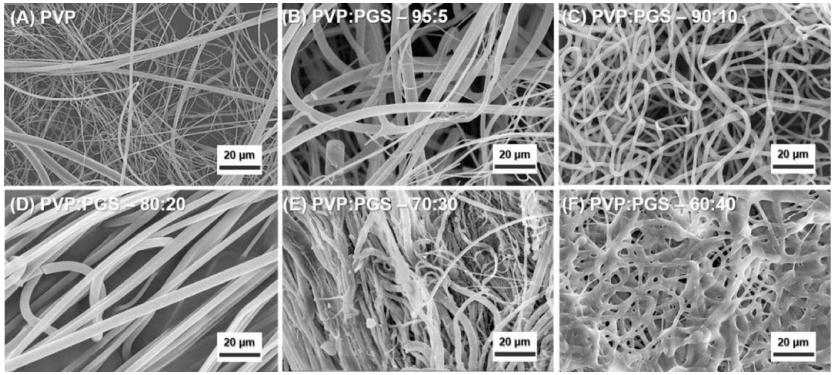

Fig. 3 SEM micrographs of 1.3 M g/mol. PVP:PGS blends, (A) pure PVP, (B) 90:10, (C) 80:20, (D) 70:30, (E) 60:40 and (F) 50:50.

alt-text: Fig 3

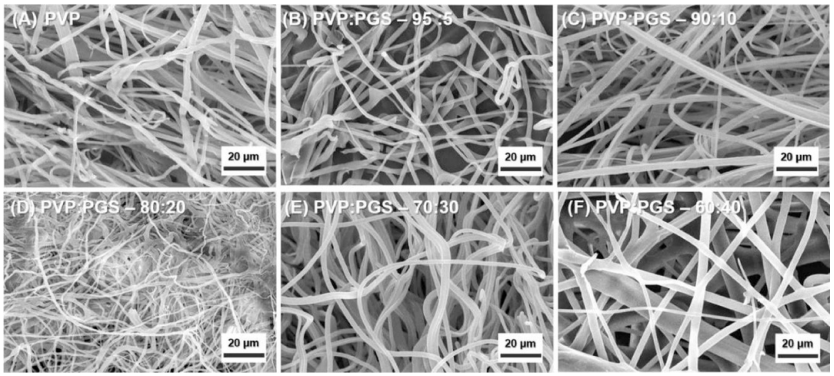

Fig. 4 SEM micrographs of 360 k g/mol PVP. PVP:PGS blends, (A) pure PVP, (B) 90:10, (C) 80:20, (D) 70:30, (E) 60:40 and (F) 50:50.

alt-text: Fig 4

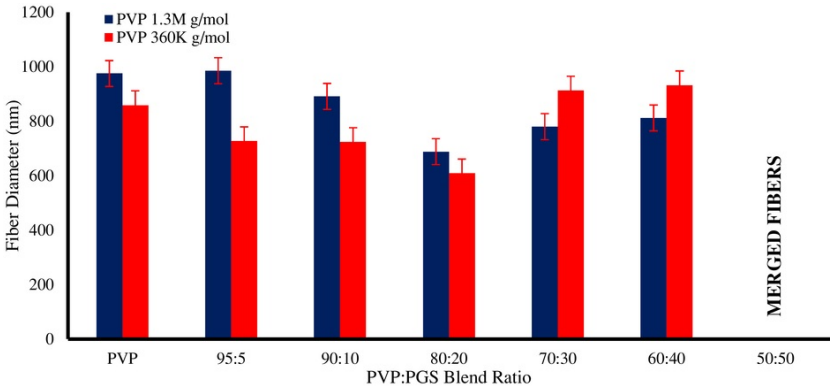

Fig. 5 Mean fiber diameter of the various PVP:PGS blends with two different molecular weight carrier PVP, 1.3 M and 360 k.

alt-text: Fig 5

3.2 Chemical characterization

ATR-FTIR was conducted to verify the synthesis of PGS. The single signal immense loop at the 1740 cm^{-1} region suggests a very saturated (double bonded) molecule of strong ester linkages (C=O). At approximately 3050 cm^{-1}, a stretch is apparent between the hydrogen (X-H) region and the broad loop forming out of a single peak at 3460 cm^{-1}, which indicates the presence of –OH groups. Two peaks are also present at approximately 2930 cm^{-1} and 2860 cm^{-1}, characteristic of C-H sp^2 and sp^3 hybridizations, respectively. The results confirm the successful synthesis of PGS and agree with previously published works [31,49].

The intense band present at 1650 cm^{-1} can be attributed to dipole (C=O) groups. Stretches at 2850 cm^{-1} can be assigned to a C-H stretch, 1420 cm^{-1} to $-CH_3$ group sp^3 hybridizations and the vibration at 1280 cm^{-1} to cyanide (CN) stretching of the PVP lactam ring [50–52]. In the composite PVP:PGS electrospun mat, the peaks from both polymers are present at different intensities with no significant shifts or new peaks present, indicative of successful blending of the two components in the fibrous mesh. The spectra of the polymers, the composite blend, glycerol, and sebacic acid are presented in Fig. 6.

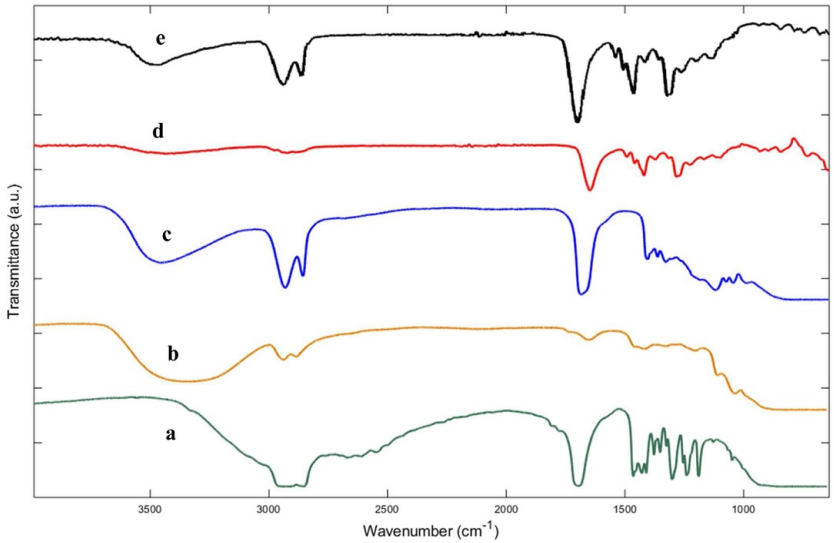

Fig. 6 ATR-FTIR spectra of (a) sebacic acid, (b) glycerol, (c) PGS gel, (d) PVP powder and (e) PVP:PGS 60:40 fibers.

alt-text: Fig 6

3.3 Surface composition

The surface composition of the electrospun mats was examined by XPS incorporating an information depth of about 10 nm. Table 2 displays the elemental ratios of each blend fibers after UV irradiation for 30 min. The surface elemental composition does not appear to be highly affected between the various composite fibers where the chemical distribution correlates to the theoretical composition values within a margin of error. No differences in the ratio profile of each blend are apparent when comparing the two distinct molecular weights of PVP. PGS ($(C_{13}H_{22}O_5)_n$) does not contain nitrogen atoms as in the case of PVP with a chemical structure of $(C_6H_9NO)_n$, making it feasible to distinguish the latter one. The presence of the N1s peak between 398–399 eV in all the blends confirming the existence of PVP within the composite fibers. In the case of blends with an increased concentration of PVP, the nitrogen content appears to be lower than the predicted values for a homogenous mixture. This depletion of PVP on the fibers' surface is due to the fiber formation process, where consecutive steps like solvent evaporation and polymer chain migration are present being dependent on the individual properties of the polymers.

Table 2 Surface chemical composition of the electrospun PVP:PGS mats at different ratios for the two distinct M_W's of PVP examined, compared to the theoretical elemental ratios.

alt-text: Table 2

PVP:PGS ~~Ratio~~ratio	Outcome	Elemental ~~Ratio~~ratio		
(w/w)	(%)	Atom (%)		
PVP 1.3_M		**C1s**	**O1s**	**N1s**
80:20	Experimental	78.7	15.0	6.3

	Theoretical	74.4	15.6	10
70:30	Experimental	70.5	21.7	7.8
	Theoretical	74.15	17.28	8.75
60:40	Experimental	75.3	17.1	7.6
	Theoretical	73.8	18.7	7.5
PVP 360 k		C1s	O1s	N1s
80:20	Experimental	64.7	26.7	8.6
	Theoretical	74.4	15.6	10
70:30	Experimental	75.2	20.1	4.7
	Theoretical	74.15	17.28	8.75
60:40	Experimental	73.0	21.8	5.2
	Theoretical	73.8	18.7	7.5

3.4 Thermal analysis

The stability and crystallinity of the PVP:PGS composite membranes were examined by DSC. The corresponding thermograms of the neat polymers, as well as the composite fibers, are illustrated in Fig. 7. The PGS thermogram indicates that the elastomer is semi-crystalline below the melting temperature (T_m) and amorphous at 37 °C. The synthesized PGS exhibits two melting temperatures, T_{m1} at 9.1 °C and a broader T_{m2} at 37.8 °C, a crystallinity point (T_c) at −~~58~~ 58 °C and a glass transition temperature (T_g) at −38.6 °C while the melting enthalpy (ΔH) was found to be 11.9 J/g for T_{m1} and 4.3 J/g for T_{m2}. The thermal behavior of the PVP powder followed the outline of a hygroscopic amorphous material with a broad endothermal effect present between 85~~ to~~ and 120 °C. Interestingly, the electrospun composite PVP:PGS mats appear to alternate the thermal properties of the materials with no apparent melting points present within the examined temperature range, suggesting chemical interactions between the PGS and PVP polymer chains. Even so, a small incline in the heat flow is apparent at the PVP endothermal effect area, which gradually decreases as the concentration of PGS increases in the composite fibers. A similar pattern has been observed from Unnisa et al. There were no distinct differences among the thermal behavior of the diverse blends of the electrospun mats [53]. Nonetheless, the T_c appeared to be present at 54.2 °C, 52.8 °C, 53.8 °C and 54.6 °C for PGS:PVP 50:50, 60:40, 70:30 and 80:20, respectively, with an intensity analogous to that of the raw PGS.

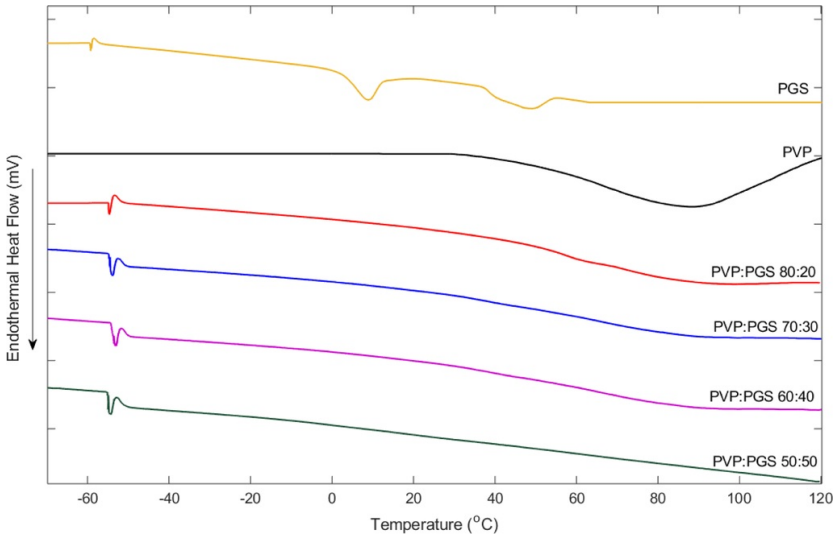

Fig. 7 Differential scanning calorimetry, first heating curves of PGS gel, PVP fibers and PVP:PGS 50:50, 60:40, 70:30 and 80:20 fiber mats.

alt-text: Fig 7

3.5 Mechanical properties

PGS has been extensively studied due to its appealing mechanical properties for soft material tissue engineering and its excellent biocompatibility. The effects that the incremental increase in the concentration of PGS has on the mechanical properties of the electrospun scaffolds is illustrated in Fig. 8. The Young's modulus (E), ultimate tensile strength (UTS) and elongation at break (ε) were obtained for the 80:20, 70:30, 60:40 and 50:50 blend ratios of PVP:PGS for the two distinct M_w of PVP examined on this study.

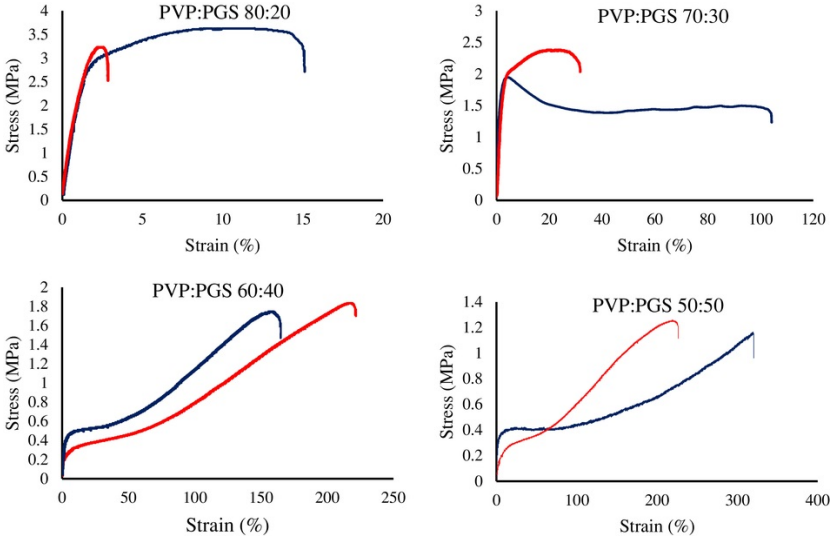

Fig. 8 Stress-strain curves of the various PVP:PGS fibrous membranes. Red: PVP 360 k g/mol, Blue: PVP 1.3 M g/mol. (For interpretation of the references to colour in this figure legend, the reader is referred to the web version of this article).

alt-text: Fig 8

For the high concentration PVP (80:20, PVP:PGS) the tensile behavior of the electrospun fibers, as expected, resembles that of neat PVP fibers with a UTS of 3.45 ± 0.3 MPa and 3.~~2~~2 ± ± 0.3 MPa for 1.3 M and 360 k g/mol PVP, respectively [54]. The stiffness of the scaffolds with low [PGS] is also apparent with ε being 14.5 ± 2.8% and 3.~~1~~1 ± 0.7% for 1.3 M and 350k g/mol PVP, respectively. Although the capacity of the material to persevere the UTS gradually decreased for increased PGS concentrations, the ε gradually increased from 106 ± 5% and 29 ± 0.7% for the 70:30 blend ratios of to 220 ± 19% and 328 ± 38% for 360 k and 1.3 M g/mol PVP, respectively (Table 3). This pattern relates not only to the PGS but also to the M_w of the PVP. Nonetheless, the ability of the electrospun fibers to withstand linear deformation decreased by increasing the PGS concentration.

Table 3 Mechanical properties of the fiber mats blends.

alt-text: Table 3

Blend ratio	Ultimate tensile stress (MPa)		Ultimate strain to failure (MPa)		Young's modulus (MPa)	
PVP (g/mol)	1.3 M	360 k	1.3 M	360 k	1.3 M	360 k
80:20	3.5 ± 0.3	3.2 ± 0.3	14.5 ± 2.8	3.1 ± 0.7	169 ± 30	170 ± 38
70:30	1.6 ± 0.1	2.1 ± 0.2	106 ± 5	29 ± 7.9	40 ± 8.4	38 ± 10
60:40	1.9 ± 0.3	1.7 ± 0.3	225 ± 15	176 ± 23	1.3 ± 0.2	2.2 ± 0.5
50:50	1.1 ± 0.1	1.7 ± 0.6	328 ± 38	220 ± 19	1.4 ± 0.6	1.4 ± 0.7

The incorporation of PGS within composite fibers has been shown to sharply decrease the E and UTS of fibers formed by stiff polymers such as collagen where the E decreased from 30.11 MPa to 4.24 MPa after incorporating the elastomer [55].

3.6 Contact angle measurements

Water contact angle (CA) measurements were obtained for the PVP:PGS electrospun mats prior and after being irradiated with UV light for 30 and 60 min. As shown in Fig. 9, an apparent increase in the static CA is apparent for the electrospun mats that were irradiated, which correlates to the exposure time. The CA of the PVP fibers was 20.2°, while the PVP:PGS was 30.4 ± 1.73° for the untreated fibers, 35.4 ± 1.06° for 30 min of UV treatment and 51.9 ± 1.98° for 60 min. PVP electrospun fibers in the literature appear to have similar values [56]. Contrarily, PGS gels CA ranges from 53 to 70°; thus, PVP considerably influences the wettability of the electrospun mats, making the composite fibers hydrophilic [56–58]. In the majority of studies, UV treatment of electrospun fibers has been shown to reduce the hydrophobicity of materials such as PCL [59] and Poly(lactic acid) [60]. However, here we observed the contrary. Poly(vinyl alcohol) UV irradiation has been shown previously to both increase and decrease the hydrophobicity of hydrogels relating to the baking temperature that is applied during the UV treatment [61]. In this study, heat was not applied at the surface of the electrospun mats during this process; as initial observations appeared to burn the scaffolds, something that could be explained due to the low melting point of PGS. Based on these observations, in conjecture, possible crosslinking between the PVP and PGS side chains that correlates to the time of exposure to UV light can be considered. This indicates that the wettability of the PVP:PGS fibers can be manipulated to an extent via UV irradiation. UV photocrosslinking of PVP via the conjugation of the molecule's monomers in an aqueous solution has been previously proven feasible for hydrogels [46]. A parametric study of the UV intensity and exposure time on the composite fibers could divulge the mechanism behind this phenomenon.

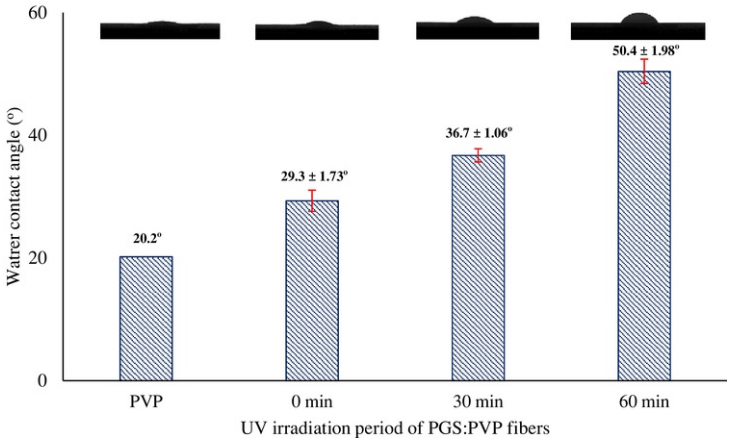

Fig. 9 Contact angle measurements in deionized water of PVP:PGS 60:40 fibers irradiated with ultraviolet light for 0, 30 and 60 min.

alt-text: Fig 9

3.7 *In vitro* biocompatibility

The UV-treated PVP:PGS fiber mats were seeded with human dermal fibroblasts to examine the cytocompatibility and attachment properties. As no differences were present in the expansion of the cells between PVP 360 k and 1.3 M g/mol, the data were merged as one group. Fig. 10 shows the fluorescence intensity that corresponds to the exponential proliferation of the cells within a week. A significant increase ($p < 0.05$) in the cell number of HDF incubated for 1 d, 3 d, 5 d, and 7 d on the PVP:PGS mats could be observed steadily, with a viability rate of above 93% for all the counted time increments. Overall, the PVP:PGS fibers with the highest concentration of PGS (60:40, PVP:PGS) appear to have the best proliferation rate. This could possibly be attributed to the fact that moderately hydrophobic polymers such as PGS have been shown to support greater attachment properties compared to hydrophilic polymers, as protein absorption is favored by hydrophobic surfaces [62]. Furthermore, the adhesion ability of the cells on a biomaterial's surface arbitrates via strong interactions between ECM proteins, such as collagen or fibrin, secreted by the cells and the chemical composition of the biomaterial's matrix [63]. Based on these preliminary results, the scaffolds do not appear to induce any apparent cytotoxic effects on HDF and show excellent biocompatibility.

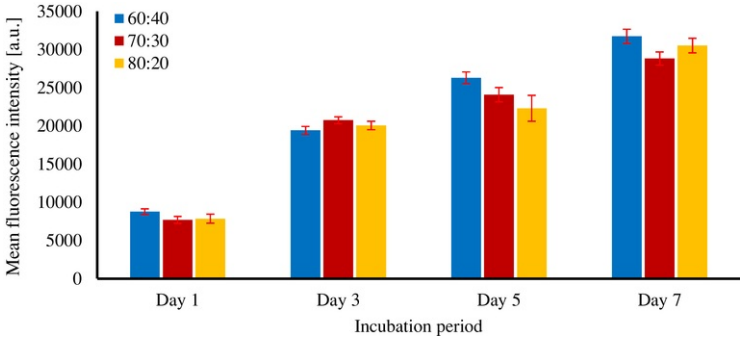

Fig. 10 Alamar blue cell viability assay of the PVP:PGS scaffolds (n=6).

alt-text: Fig 10

The SEM micrographs shown in Fig. 11 indicate that the seeded fibroblasts carry a good polygonal morphology for PVP:PGS concentrations of 80:20, 70:30 and 60:40 — characteristic of healthy fibroblasts — compared to the round morphology apparent for PVP:PGS 50:50. Cell attachment to the fiber surface was visibly apparent on the day of inoculation, with good surface interactions present between the adherent cells and the electrospun fibers. The cells appear to have spread quickly over the electrospun mats and were capable of expanding and covering the scaffolds within 5 days of inoculation. No cellular expansion was present for the 50:50 PVP:PGS blends, which formed a gel, demonstrating the benefits of an ECM-like architecture towards the expansion of cells.

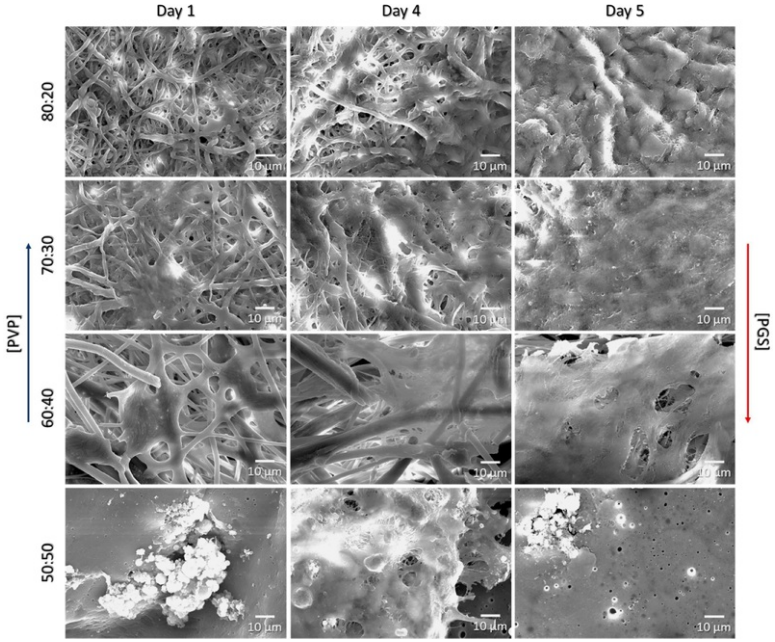

Fig. 11 SEM micrographs displaying the fibroblast (HDF-TERT) morphology on the electrospun scaffolds, after 1, 4 and 5 days of incubation. PVP:PGS 80:20; 70:30; 60:40 and 50:50 (w/w). PVP 360 k g/mol. Scale bar 10 µm.

alt-text: Fig 11

Thus, PVP:PGS fibers are worth considering as a possible wound dressing for skin regeneration. Further work needs to be performed to examine the cellular attachment mechanism, as well as possible inflammation.

4 Conclusions

In this study, for the first time, PVP:PGS fibers were fabricated via electrospinning as promising candidates for mechanically tunable and biocompatible skin tissue constructs. The morphology, physiochemical properties, mechanics, wettability and biocompatibility, were examined.

As the PGS to PVP ratio increased, so did the elongation at break of the corresponding scaffolds, while the elastic modulus and ultimate tensile strength gradually decreased. The mechanical properties of the fiber mats improved significantly with the addition of PGS; however, fiber uniformity was not preserved at higher proportions. This study does not come without its limitations; further work needs to be conducted in order to understand the surface chemistry of the developed constructs, the mechanisms behind the effect that UV carries to the wettability and degradability of the PVP:PGS scaffolds preventing rapid degradation.

The present study provides valuable input in the ability of PGS fibers to tune the behavior of PVP just by increasing its concentration within the blend. This new composite system, focusing on potential skin regeneration, shows good potential for further investigations focusing on soft tissue engineering applications.

Conflicts of interest

None.

Funding

None.

Ethical approval

Not required.

Acknowledgments

We would like to thank Dr. Junxi Wu from the Centre of Cardiovascular Science of The University of Edinburgh for donating the cell-line used for the viability testing. We thank Professor Vasileios Koutsos and Dr. Colin Robert of The University of Edinburgh for their valued suggestions. The authors also thank Dr. Coinneach Dover and Dr. Mike Davidson of The University of Edinburgh for providing access and training on the water contact angle measurement and FTIR equipment, respectively. We would also like to thank Fergus Dingwall, Mariia Zakharova and Jae Hoon Kwon of The University of Edinburgh for their appreciated laboratory assistance.

Supplementary materials

Supplementary material associated with this article can be found, in the online version, at doi:10.1016/j.medengphy.2019.06.009.

References

[1] F. Groeber, M. Holeiter, M. Hampel, S. Hinderer and K. Schenke-Layland, Skin tissue engineering - *In vivo* and *in vitro* applications, *Adv Drug Deliv Rev* **63**, 2011, 352–366, https://doi.org/10.1016/j.addr.2011.01.005.

[2] R.A. Franco, Y.-K. Min, H.-M. Yang and B.-T. Lee, Fabrication and biocompatibility of novel bilayer scaffold for skin tissue engineering applications, *J Biomater Appl* **27**, 2013, 605–615, https://doi.org/10.1177/0885328211416527.

[3] M. Bacakova, J. Musilkova, T. Riedel, D. Stranska, E. Brynda, L. Bacakova, et al., The potential applications of fibrin-coated electrospun polylactide nanofibers in skin tissue engineering, *Int J Nanomedicine* **11**, 2016, 771, https://doi.org/10.2147/IJN.S99317.

[4] K. Vig, A. Chaudhari, S. Tripathi, S. Dixit, R. Sahu, S. Pillai, et al., Advances in skin regeneration using tissue engineering, *Int J Mol Sci* **18**, 2017, https://doi.org/10.3390/ijms18040789.

[5] Y. Liu, Y. Zheng and B. Hayes, Degradable, absorbable or resorbable—what is the best grammatical modifier for an implant that is eventually absorbed by the body?, *Sci China Mater* **60**, 2017, 377–391, https://doi.org/10.1007/s40843-017-9023-9.

[6] H. Debels, M. Hamdi, K. Abberton and W. Morrison, Dermal matrices and bioengineered skin substitutes, *Plast Reconstr Surg Glob Open* **3**, 2015, e284, https://doi.org/10.1097/GOX.0000000000000219.

[7] R. Rai, M. Tallawi, A. Grigore and A.R. Boccaccini, Synthesis, properties and biomedical applications of poly(glycerol sebacate) (PGS): a review, *Prog Polym Sci* **37**, 2012, 1051–1078,

https://doi.org/10.1016/j.progpolymsci.2012.02.001.

[8] Y. Wang, G.A. Ameer, B.J. Sheppard and R. Langer, A tough biodegradable elastomer, *Nat Biotechnol* **20**, 2002, 602–606, https://doi.org/10.1038/nbt0602-602.

[9] J.M. Kemppainen and S.J. Hollister, Tailoring the mechanical properties of 3D-designed poly(glycerol sebacate) scaffolds for cartilage applications, *J Biomed Mater Res - Part A* **94**, 2010, 9–18, https://doi.org/10.1002/jbm.a.32653.

[10] Y. Wang, G.A. Ameer, B.J. Sheppard and R. Langer, A tough biodegradable elastomer, *Nat Biotechnol* **20**, 2002, 602–606, https://doi.org/10.1038/nbt0602-602.

[11] F. Yi and D.A. La Van, Poly(glycerol sebacate) nanofiber scaffolds by core/shell electrospinning, *Macromol Biosci* **8**, 2008, 803–806, https://doi.org/10.1002/mabi.200800041.

[12] Y. Li, W. Huang, W.D. Cook and Q. Chen, A comparative study on poly(xylitol sebacate) and poly(glycerol sebacate): mechanical properties, biodegradation and cytocompatibility, *Biomed Mater* **8**, 2013, https://doi.org/10.1088/1748-6041/8/3/035006.

[13] W.H. Tham, M.U. Wahit, M.R. Abdul Kadir, T.W. Wong and O. Hassan, Polyol-based biodegradable polyesters: a short review, *Rev Chem Eng* 2016, https://doi.org/10.1515/revce-2015-0035.

[14] I.H. Jaafar, M.M. Ammar, S.S. Jedlicka, R.A. Pearson and J.P. Coulter, Spectroscopic evaluation, thermal, and thermomechanical characterization of poly(glycerol-sebacate) with variations in curing temperatures and durations, *J Mater Sci* **45**, 2010, 2525–2529, https://doi.org/10.1007/s10853-010-4259-0.

[15] Y. Wang, Y.M. Kim and R. Langer, In vivo degradation characteristics of poly(glycerol sebacate), *J Biomed Mater Res* **66A**, 2003, 192–197, https://doi.org/10.1002/jbm.a.10534.

[16] D. Dippold, M. Tallawi, S. Tansaz, J.A. Roether and A.R. Boccaccini, Novel electrospun poly(glycerol sebacate)-zein fiber mats as candidate materials for cardiac tissue engineering, *Eur Polym J* **75**, 2016, 504–513, https://doi.org/10.1016/j.eurpolymj.2015.12.030.

[17] M. Tallawi, D.C. Zebrowski, R. Rai, J.A. Roether, D.W. Schubert, M. El Fray, et al., Poly(Glycerol sebacate)/poly(butylene succinate-butylene Dilinoleate) fibrous scaffolds for cardiac tissue engineering, *Tissue Eng Part C Methods* **21**, 2015, 585–596, https://doi.org/10.1089/ten.tec.2014.0445.

[18] M. Tallawi, D. Dippold, R. Rai, D. D'Atri, J.A. Roether, D.W. Schubert, et al., Novel PGS/PCL electrospun fiber mats with patterned topographical features for cardiac patch applications, *Mater Sci Eng C* **69**, 2016, 569–576, https://doi.org/10.1016/j.msec.2016.06.083.

[19] R. Khosravi, C.A. Best, R.A. Allen, C.E.T. Stowell, E. Onwuka, J.J. Zhuang, et al., Long-Term functional efficacy of a novel electrospun poly(glycerol sebacate)-based arterial graft in mice, *Ann Biomed Eng* **44**, 2016, 2402–2416, https://doi.org/10.1007/s10439-015-1545-7.

[20] P.M. Crapo, J. Gao and Y. Wang, Seamless tubular poly(glycerol sebacate) scaffolds: high-yield fabrication and potential applications, *J Biomed Mater Res - Part A* **86**, 2008, 354–363, https://doi.org/10.1002/jbm.a.31598.

[21] C.G. Jeong and J. Hollister Scott, A comparison of the influence of material on in vitro cartilage tissue engineering with PCL, PGS, and POC 3D scaffold architecture seeded with chondrocytes, *Biomaterials* **31**, 2010, 4304–4312, https://doi.org/10.1016/j.biomaterials.2010.01.145.

[22] Allen R.A., Wu W., Yao M., Dutta D., Duan X., Timothy N., et al. Implantation in a rat model2015;35:1–18. doi:10.1016/j.biomaterials.2013.09.081.Nerve.

[23] C.A. Sundback, J.Y. Shyu, Y. Wang, W.C. Faquin, R.S. Langer, J.P. Vacanti, et al., Biocompatibility analysis of poly(glycerol sebacate) as a nerve guide material, *Biomaterials* **26**, 2005, 5454–5464, https://doi.org/10.1016/j.biomaterials.2005.02.004.

[24] L. Taylor, K. Arnér, M. Kolewe, C. Pritchard, G. Hendy, R. Langer, et al., Seeing through the interface: poly(ε-Caprolactone) surface modification of poly(glycerol-co-sebacic acid) membranes in adult porcine retinal explants, *J Tissue Eng Regen Med* **11**, 2017, 2349–2358, https://doi.org/10.1002/term.2135.

[25] W.L. Neeley, S. Redenti, H. Klassen, S. Tao, T. Desai, M.J. Young, et al., A microfabricated scaffold for retinal progenitor cell grafting, *Biomaterials* **29**, 2008, 418–426, https://doi.org/10.1016/j.biomaterials.2007.10.007.

[26] S. Redenti, W.L. Neeley, S. Rompani, S. Saigal, J. Yang, H. Klassen, et al., Engineering retinal progenitor cell and scrollable poly(glycerol-sebacate) composites for expansion and subretinal transplantation, *Biomaterials*

30, 2009, 3405–3414, https://doi.org/10.1016/j.biomaterials.2009.02.046.

[27] M. Frydrych, S. Román, S. Macneil and B. Chen, Biomimetic poly(glycerol sebacate)/poly(l-lactic acid) blend scaffolds for adipose tissue engineering, *Acta Biomater* **18**, 2015, 40–49, https://doi.org/10.1016/j.actbio.2015.03.004.

[28] X. Zhang, C. Jia, X. Qiao, T. Liu and K. Sun, Porous poly(glycerol sebacate) (PGS) elastomer scaffolds for skin tissue engineering, *Polym Test* **54**, 2016, 118–125, https://doi.org/10.1016/j.polymertesting.2016.07.006.

[29] X. Zhang, C. Jia, X. Qiao, T. Liu and K. Sun, Silk fibroin microfibers and chitosan modified poly (glycerol sebacate) composite scaffolds for skin tissue engineering, *Polym Test* **62**, 2017, 88–95, https://doi.org/10.1016/j.polymertesting.2017.06.012.

[30] Z.J. Sun, C. Chen, M.Z. Sun, C.H. Ai, X.L. Lu, Y.F. Zheng, et al., The application of poly (glycerol-sebacate) as biodegradable drug carrier, *Biomaterials* **30**, 2009, 5209–5214, https://doi.org/10.1016/j.biomaterials.2009.06.007.

[31] B. Yang, W. Lv and Y. Deng, Drug loaded poly(glycerol sebacate) as a local drug delivery system for the treatment of periodontal disease, *RSC Adv* **7**, 2017, 37426–37435, https://doi.org/10.1039/C7RA02796F.

[32] M. Masoudi Rad, S. Nouri Khorasani, L. Ghasemi-Mobarakeh, M.P. Prabhakaran, M.R. Foroughi, M. Kharaziha, et al., Fabrication and characterization of two-layered nanofibrous membrane for guided bone and tissue regeneration application, *Mater Sci Eng C* **80**, 2017, 75–87, https://doi.org/10.1016/j.msec.2017.05.125.

[33] A.P. Hurt, G. Getti and N.J. Coleman, Bioactivity and biocompatibility of a chitosan-tobermorite composite membrane for guided tissue regeneration, *Int J Biol Macromol* **64**, 2014, 11–16, https://doi.org/10.1016/j.ijbiomac.2013.11.020.

[34] A. Nadim, S.N. Khorasani, M. Kharaziha and S.M. Davoodi, Design and characterization of dexamethasone-loaded poly (glycerol sebacate)-poly caprolactone/gelatin scaffold by coaxial electro spinning for soft tissue engineering, *Mater Sci Eng C* **78**, 2017, 47–58, https://doi.org/10.1016/j.msec.2017.04.047.

[35] N. Radacsi, F.D. Campos, C.R.I. Chisholm and K.P. Giapis, Spontaneous formation of nanoparticles on electrospun nanofibres, *Nat Commun* 2018, https://doi.org/10.1038/s41467-018-07243-5.

[36] E.M. Jeffries, R.A. Allen, J. Gao, M. Pesce and Y. Wang, Highly elastic and suturable electrospun poly(glycerol sebacate) fibrous scaffolds, *Acta Biomater* **18**, 2015, 30–39, https://doi.org/10.1016/j.actbio.2015.02.005.

[37] G. Coativy, M. Misra and A.K. Mohanty, Synthesis of shape memory Poly(glycerol sebacate)-Stearate polymer, *Macromol Mater Eng* **302**, 2017, 1–6, https://doi.org/10.1002/mame.201600294.

[38] J. Hu, D. Kai, H. Ye, L. Tian, X. Ding, S. Ramakrishna, et al., Electrospinning of poly (glycerol sebacate)-based nanofibers for nerve tissue engineering, *Mater Sci Eng C* **70**, 2017, 1089–1094.

[39] S. Sant and A. Khademhosseini, Fabrication and characterization of tough elastomeric fibrous scaffolds for tissue engineering applications, In: *Proceedings of the annual international conference on IEEE engineering in medicine and biology society, EMBC'10,* 2010, 3546–3548, https://doi.org/10.1109/IEMBS.2010.5627486.

[40] R. Ravichandran, J.R. Venugopal, S. Sundarrajan, S. Mukherjee and S. Ramakrishna, Poly(Glycerol sebacate)/gelatin core/shell fibrous structure for regeneration of myocardial infarction, *Tissue Eng Part A* **17**, 2011, 1363–1373, https://doi.org/10.1089/ten.tea.2010.0441.

[41] M. Kharaziha, M. Nikkhah, S.R. Shin, N. Annabi, N. Masoumi, A.K. Gaharwar, et al., PGS:gelatin nanofibrous scaffolds with tunable mechanical and structural properties for engineering cardiac tissues, *Biomaterials* **34**, 2013, 6355–6366, https://doi.org/10.1016/j.biomaterials.2013.04.045.

[42] B. Xu, Y. Li, C. Zhu, W.D. Cook, J. Forsythe and Q. Chen, Fabrication, mechanical properties and cytocompatibility of elastomeric nanofibrous mats of poly(glycerol sebacate), *Eur Polym J* **64**, 2015, 79–92, https://doi.org/10.1016/j.eurpolymj.2014.12.008.

[43] Z.R. You, M.H. Hu, H.Y. Tuan-Mu and J.J. Hu, Fabrication of poly(glycerol sebacate) fibrous membranes by coaxial electrospinning: influence of shell and core solutions, *J Mech Behav Biomed Mater* **63**, 2016, 220–231, https://doi.org/10.1016/j.jmbbm.2016.06.022.

[44] C.Y. Kao, T.C. Lo and W.C. Lee, Influence of polyvinylpyrrolidone on the hydrophobic properties of partially porous poly(styrene-divinylbenzene) particles for biological applications, *J Appl Polym Sci* **87**, 2003, 1818–1824, https://doi.org/10.1002/app.11653.

[45] A. Ní Annaidh, K. Bruyère, M. Destrade, M.D. Gilchrist and M. Otténio, Characterization of the anisotropic mechanical properties of excised human skin, *J Mech Behav Biomed Mater* **5**, 2012, 139–148, https://doi.org/10.1016/j.jmbbm.2011.08.016.

[46] L.C. Lopérgolo, A.B. Lugão and L.H. Catalani, Direct UV photocrosslinking of poly(N-vinyl-2-pyrrolidone) (PVP) to produce hydrogels, *Polymer (Guildf)* **44**, 2003, 6217–6222, https://doi.org/10.1016/S0032-3861(03)00686-4.

[47] J. Heo, R.H. Koh, W. Shim, H.D. Kim, H.G. Yim and N.S. Hwang, Riboflavin-induced photo-crosslinking of collagen hydrogel and its application in meniscus tissue engineering, *Drug Deliv Transl Res* **6**, 2016, 148–158, https://doi.org/10.1007/s13346-015-0224-4.

[48] British Standards Institution. Plastics. Part 3. Test conditions for films and sheets : determination of tensile properties. BSI; 1996.

[49] R. Rai, M. Tallawi, A. Grigore and A.R. Boccaccini, Synthesis, properties and biomedical applications of poly(glycerol sebacate) (PGS): a review, *Prog Polym Sci* **37**, 2012, 1051–1078, https://doi.org/10.1016/j.progpolymsci.2012.02.001.

[50] Y.J. Song, M. Wang, X.Y. Zhang, J.Y. Wu and T. Zhang, Investigation on the role of the molecular weight of polyvinyl pyrrolidone in the shape control of highyield silver nanospheres and nanowires, *Nanoscale Res Lett* **9**, 2014, 1–8, https://doi.org/10.1186/1556-276X-9-17.

[51] A.M. Abdelghany, M.S. Mekhail, E.M. Abdelrazek and M.M. Aboud, Combined DFT/FTIR structural studies of monodispersed PVP/Gold and silver nano particles, *J Alloys Compd* **646**, 2015, 326–332, https://doi.org/10.1016/j.jallcom.2015.05.262.

[52] J. Li, K. Inukai, Y. Takahashi, A. Tsuruta and W. Shin, Thin film coating with highly dispersible barium titanate-polyvinylpyrrolidone nanoparticles, *Materials (Basel)* **11**, 2018, 712, https://doi.org/10.3390/ma11050712.

[53] C. Nusrath Unnisa, S. Chitra, S. Selvasekarapandian, S. Monisha, G. Nirmala Devi, V. Moniha, et al., Development of poly(glycerol suberate) polyester (PGS)–PVA blend polymer electrolytes with NH4SCN and its application, *Ionics (Kiel)* 2018, https://doi.org/10.1007/s11581-018-2466-x.

[54] S. Huang, L. Zhou, M.-C. Li, Q. Wu, Y. Kojima and D. Zhou, Preparation and properties of electrospun poly (Vinyl pyrrolidone)/cellulose nanocrystal/silver nanoparticle composite fibers, *Materials (Basel)* **9**, 2016, 523, https://doi.org/10.3390/ma9070523.

[55] R. Ravichandran, Cardiogenic differentiation of mesenchymal stem cells on elastomeric poly (glycerol sebacate)/collagen core/shell fibers, *World J Cardiol* **5**, 2013, 28, https://doi.org/10.4330/wjc.v5.i3.28.

[56] L. Wang, C. Zhang, H.M.D. Wang, Z. Ahmad, J.S. Li and M.W. Chang, High throughput engineering and use of multi-fiber composite matrices for controlled active release, *Mater Today Commun* **17**, 2018, 53–59, https://doi.org/10.1016/j.mtcomm.2018.08.011.

[57] A.K. Gaharwar, A. Patel, A. Dolatshahi-Pirouz, H. Zhang, K. Rangarajan, G. Iviglia, et al., Elastomeric nanocomposite scaffolds made from poly(glycerol sebacate) chemically crosslinked with carbon nanotubes, *Biomater Sci* **3**, 2015, 46–58, https://doi.org/10.1039/C4BM00222A.

[58] H. Shi, Q. Gan, X. Liu, Y. Ma, J. Hu, Y. Yuan, et al., Poly(glycerol sebacate)-modified polylactic acid scaffolds with improved hydrophilicity, mechanical strength and bioactivity for bone tissue regeneration, *RSC Adv* **5**, 2015, 79703–79714, https://doi.org/10.1039/c5ra13334c.

[59] R. Augustine, A. Saha, V.P. Jayachandran, S. Thomas and N. Kalarikkal, Dose-dependent effects of gamma irradiation on the materials properties and cell proliferation of electrospun polycaprolactone tissue engineering scaffolds, *Int J Polym Mater Polym Biomater* **64**, 2015, 526–533, https://doi.org/10.1080/00914037.2014.977900.

[60] T.A.M. Valente, D.M. Silva, P.S. Gomes, M.H. Fernandes, J.D. Santos and V. Sencadas, Effect of sterilization methods on electrospun poly(lactic acid) (PLA) fiber alignment for biomedical applications, *ACS Appl Mater Interfaces* **8**, 2016, 3241–3249, https://doi.org/10.1021/acsami.5b10869.

[61] Musskaya O.N., Kulak A.I., Krut V.K., Ulasevich S.A., Lesnikovich L.A., Suchodub L.F.Composite films based on hydroxyapatite and polyvinyl alcohol2015;7:1–4.

[62] Ifkovits J.L., Devlin J.J., Eng G., Martens T.P., Vunjak- G., Burdick J.A.Biodegradable fibrous scaffolds with tunable properties formed from photocrosslinkable Poly(glycerol sebacate)2010;1:1878–92.

doi:10.1021/am900403k.Biodegradable.

[63] E.S. Place, N.D. Evans and M.M. Stevens, Complexity in biomaterials for tissue engineering, *Nat Mater* **8**, 2009, 457–470, https://doi.org/10.1038/nmat2441.

Appendix. Supplementary materials

Multimedia Component 1

alt-text: Image, application 1

Multimedia Component 2

alt-text: Image, application 2

Graphical abstract

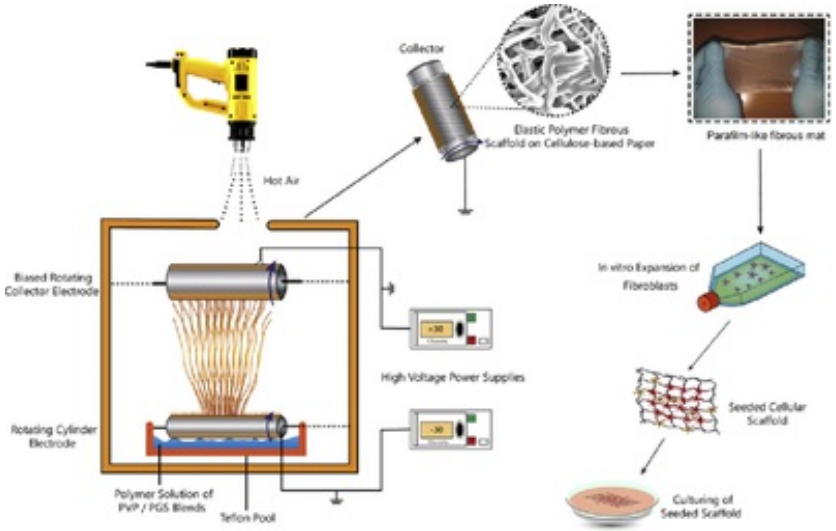

alt-text: Image, graphical abstract

Highlights

- High-throughput production of fibers using a nozzle-free electrospinning device.
- Tunable mechanical properties attainable by adjusting the blend ratio [PVP:PGS] and the PVP's molecular weight.
- Manipulation of the composite fibrous mats' wettability properties via UV irradiation.

Queries and Answers

Query: Please confirm that givennames and surnames have been identified correctly.

Answer: Yes

Query: Fig. 8 has been submitted as colour images; however, the captions have been reworded to ensure that they are meaningful when your article is reproduced both in colour and in black and white. Please check and correct if necessary.

Answer: I approve the changes you made

Query: Please provide journal title in Refs. [61,62].

Answer: [61] O.N. Musskaya, A.I. Kulak, V.K. Krut'ko, S.A. Ulasevich, L.A. Lesnikovich, L.F. Suchodub, Composite Films Based on Hydroxyapatite and Polyvinyl Alcohol, *J Nanoelectron Optoe* **7,** 2015, 01022(4pp) DOI:
10.13140/RG.2.1.3430.1042

[62] J.L. Ifkovits, J.J. Devlin, G. Eng, T.P. Martens, G., Vunjak-,Novakovic, and J.A. Burdick, Biodegradable fibrous scaffolds with tunable properties formed from photo-cross-linkable poly(glycerol sebacate) *ACS Appl Mater Interfaces, **1,** 2009,* 1878-1886, https://doi.org/10.1021/am900403k